Reactive & Functional Polymers 72 (2012) 420–426

Contents lists available at SciVerse ScienceDirect

Reactive & Functional Polymers

journal homepage: www.elsevier.com/locate/react

Cellulose acetate-poly{[9,9-bis(6′-*N*,*N*,*N*-trimethylammonium) hexyl]fluorene-phenylene} bromide blends: Preparation, characterization and transport properties

A.J.M. Valente [a,*], H.D. Burrows [a], J.N.P.L. Gomes [a], R.F.P. Pereira [a], D. Cerqueira [b], A. Jiménez [c], N. Burgos [c], C. Morán [a], R. Mallavia [d], G.R. Filho [e]

[a] Department of Chemistry, University of Coimbra, 3004-535 Coimbra, Portugal
[b] Instituto de Ciências Ambientais e Desenvolvimento Sustentável, Universidade Federal da Bahia, Rua Prof. José Seabra, S/N, CEP 47805-100 Barreiras, Bahia, Brazil
[c] Department of Analytical Chemistry, Nutrition and Food Sciences, University of Alicante, PO Box 99, 03080 Alicante, Spain
[d] Instituto de Biologia Molecular y Celular, Universidad Miguel Hernández, Elche 03202, Alicante, Spain
[e] Instituto de Química, Universidade Federal de Uberlândia, Av. João Naves de Ávila 2121, CEP 38400-902, Cx. P. 593 Uberlândia, Minas Gerais, Brazil

ARTICLE INFO

Article history:
Received 27 February 2012
Accepted 31 March 2012
Available online 11 April 2012

Keywords:
Cellulose acetate
Polyfluorene
Conjugated polyelectrolyte
Polymerization degree
Blend

ABSTRACT

The preparation of cellulose acetate-poly-(9,9-bis(6′-*N*,*N*,*N*-trimethylammonium)-hexyl-fluorene phenylene) bromide (HTMA-PFP) blend films by solvent casting from a dispersion is reported. Films were characterized by UV–visible spectroscopy, SEM, electrical conductivity, TGA and DSC. It was found that morphological and physical chemical properties of blends were dependent both on the solvent and the degree of polymerization of cellulose acetate. The fluorescence properties of different blends were evaluated by fluorescence microscopy and it was shown that they are dependent on the structural properties of the blend as well as the aggregation level of the polyfluorene. Release kinetics of HTMA-PFP, incorporated into blend films, in SDS aqueous solutions have been studied and are discussed on the basis of the Korsmeyer–Peppas equation.

1. Introduction

Ionic conjugated polyelectrolytes (CPs) are important materials as a consequence of their impact in the development of areas related to chemical [1,2] and biological [3,4] sensors, charge injection and transport layers [5]. They also demonstrate potential in areas including photovoltaic systems and light emitting diodes (LEDs) [5–7]. These ionic conjugated polymers are also relevant for applications in self-assembly [8] and for film preparation using solvent based methodologies, such as inkjet and screen printing [9]. Fluorene-based polymers show particular potential for these applications because of their blue emission and high luminescence yields [10], and, in addition, they have rigid rod structures which provide the possibility of forming nematic liquid crystalline phases [11]. However, conjugated polyelectrolytes containing the fluorene moiety tend to aggregate in aqueous solutions, leading to interchain interactions which greatly reduce luminescence yields [12]. Further, the solubility of polyfluorene based systems in water is poor. An interesting approach which has been used to increase solubility in water and, consequently, to find out the fluorescent and conductance properties of CPs is through the addition of ionic or non-ionic surfactants [13–15].

An alternative approach is the use of CPs as polymer blend films. The use of conjugated polymers in solid matrices based on cellulose has been reported for optoelectronic and sensing purposes [16,17]. In the present work, we report the preparation and characterization of films of cellulose acetate and poly-(9,9-bis(6′-*N*,*N*,*N*-trimethylammonium)-hexyl-fluorene phenylene) bromide (HTMA-PFP) blends. Cellulose acetate is a well-known polymer derived from cellulose, with neutral properties and high capacity for transparent film formation. Applications include optical devices [18,19] and membrane separation [20–22]. Cellulose acetate produces porous structures [23] and its properties are dependent on the acetylation degree. This affects a number of key structural properties, such as the polymer crystallinity, and solubility in various solvents [24,25].

In this paper, the immobilization of a cationic poly(fluorene-phenylene), poly{[9,9-bis(6′-*N*,*N*,*N*-trimethylammonium) hexyl] fluorene-phenylene} bromide (HTMA-PFP), into a cellulose acetate film has been carried out. The effect of the acetylation degree, molecular weight and solvent on the morphological, thermal, optical and conductivity properties of the blends is discussed. The desorption kinetics of the HTMA-PFP, from the blend film in the

* Corresponding author. Tel.: +351 239 854459; fax: +351 239 827703.
E-mail address: avalente@ci.uc.pt (A.J.M. Valente).

1381-5148/$ - see front matter © 2012 Elsevier Ltd. All rights reserved.
http://dx.doi.org/10.1016/j.reactfunctpolym.2012.03.014

presence of sodium dodecyl sulfate are also evaluated and discussed.

2. Experimental

2.1. Materials

Two different batches of cellulose acetate were used: commercial cellulose acetate (CA1, Aldrich, number average molecular weight – M_n 30,000 Da, repeat unit molecular weight, 279 g mol^{-1}, degree of polymerization – DP 107.5) and cellulose acetate synthesized from sugarcane bagasse, provided by Usina Caeté, from Delta, Minas Gerais, Brazil (CA2, M_n 16,900 Da, repeat unit molecular weight, 287.4 g mol^{-1}, DP 59), according to the methodology previously described [26]. The degree of substitution (DS) of cellulose acetates was determined by NMR spectroscopy following a procedure reported by Cerqueira et al. [27], and gave values equal to 2.4 and 2.6, respectively.

The cationic conjugated polyelectrolyte poly-(9,9-bis(6′-*N*,*N*,*N*-trimethylammonium)-hexyl-fluorene phenylene) bromide (HTMA-PFP, M_n 24,315 g mol^{-1}, repeat unit molecular weight, 694.71 g mol^{-1}, DP 35.0-based on PS calibration), Scheme 1, was obtained by treating the neutral polymer poly(9,9-bis(6′-hexylbromide)-fluorene phenylene), synthesized by Suzuki coupling reaction with Pd(II) as catalyst, with gas-phase trimethylamine by following a procedure described elsewhere [28].

All solvents THF, chloroform and methanol have been supplied from Riedel-de Häen.

Blend films were prepared by initially dissolving cellulose acetate in the solvent and stirring for 24 h to ensure homogeneity. HTMA-PFP was then added to the solution, as a powder (B1–B3) or solution (B4), and left stirring for further 2 h. The concentrations of CA and HTMA-PFP in the blend solution are 8.8% w/v and 0.18% w/v, respectively, corresponding to a percentage of 2% (w/w cellulose acetate/HTMA-PFP). The solution was then deposited as a film on a flat glass support using a Simex automatic film applicator. After complete evaporation of the solvent at room temperature, the membrane was removed from the glass support with the help of water. Four different blends were prepared: (i) CA1 + HTMA-PFP in THF (B1); (ii) CA1 + HTMA-PFP in $CHCl_3$ (B2); (iii) CA2 + HTMA-PFP in $CHCl_3$ (B3); and (iv) CA1 in $CHCl_3$ + HTMA-PFP in CH_3OH, with a final mixture solvent of 5% v($CHCl_3$)/v(CH_3OH) (B4). Thicknesses of membranes were measured at 25 °C using a Mitutoyo micrometer (±0.001 mm) and are equal to 0.026(±0.003), 0.025(±0.002), 0.023(±0.002) and 0.023(±0.002) mm, respectively. The first three blends were prepared to check the effect of the substitution degree of cellulose acetate and solvent on their properties. Organic solvents will increase the solubility of the conjugated polyelectrolytes by decreasing interchain and intrachain hydrophobic interactions and thus decreasing the self-assembly [29]. The influence of the initial solubilization of the polyelectrolyte [30] on the blend structure and properties will be considered using blend B4.

Cellulose acetate films, without HTMA-PFP, were prepared using the same solvent formulations for comparison.

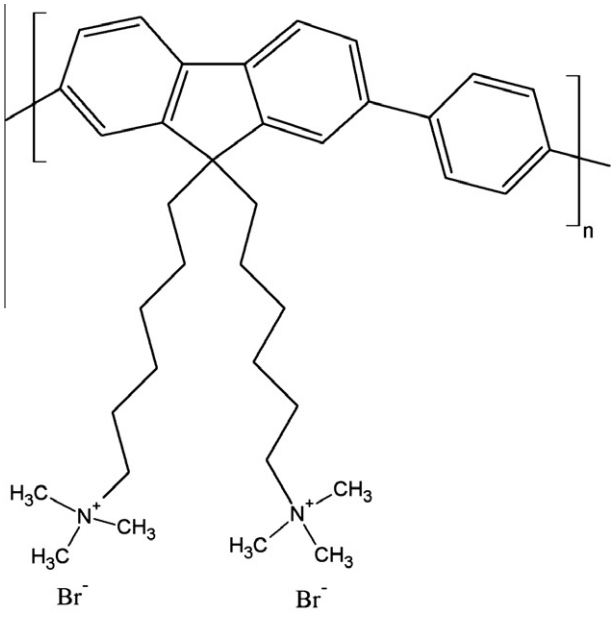

Scheme 1. Structure of the poly{[9,9-bis(6′-*N*,*N*,*N*-trimethylammonium) hexyl]fluorene-phenylene} bromide.

2.2. Methods

The incorporation of HTMA-PFP into cellulose acetate was monitored by UV–vis spectroscopy using a Shimadzu V-2450 spectrophotometer. The spectra were obtained on films directly inserted in the cell compartment, and they were studied over the wavelength range 200–600 nm, using a bandwidth of 1 nm.

The surface morphologies of blend films were analyzed by scanning electron and fluorescence microscopies (SEM and FM). SEM was carried out with a JEOL model 5310 scanning microscope operating under low vacuum, using a 20 kV potential. For FM, films were examined with an Olympus BX51 M microscope equipped with a UV-mercury lamp (100 W Ushio Olympus) and a filter set type U-MNU2 (360–370 nm excitation and 400 nm dichromatic mirror). Films were observed using an Olympus 10×/0.10 objective lens (∞/−/FN22). Images were digitalized on a computer through a video camera (Olympus digital camera DP70) and they were analyzed with an image processor (Olympus DP Controller 2.1.1.176, Olympus DP Manager 2.1.1.158 – Olympus). All observations were carried out at 20.0 (±0.1) °C.

Thermogravimetric tests (TGA) were performed on a TGA/SDTA 851 Mettler Toledo thermal analyzer. Samples were heated from room temperature up to 500 °C at 10 °C min^{-1} under nitrogen atmosphere (50 cm^3 min^{-1}).

DSC tests were carried out on a TA Instruments DSC Q2000 (New Castle, DE, USA) under a dry nitrogen gas flow rate of 50 mL min^{-1}. Samples were sealed in aluminum pans and subjected to a first heating at 10 °C min^{-1} (in order to erase the thermal history) from −60 °C up to the initial of degradation process (310 °C for CA2 blends and 270 °C for CA1 blends), followed by cooling at 10 °C min^{-1} to −60 °C and further heating at 10 °C min^{-1} up to degradation. Sample weights of about 3 mg were used in all cases. The glass transition temperature (T_g) was determined in the second heating scan as the inflection point in the region where a shift in the signal baseline was detected.

Electrical conductivity measurements were carried out using a Wayne Kerr LCR 4265 system, at 1 kHz, by following the methodology described elsewhere [31].

2.3. Desorption kinetics

The assessment on the type of incorporation of HTMA-PFP into cellulose acetate matrices and its effect on transport properties have been carried out through the analysis of the polyelectrolyte desorption to aqueous solutions of the anionic surfactant (sodium dodecyl sulfate, Aldrich), at concentrations below and above the critical micelle concentration (8.3 mM [32]). HTMA-PFP desorption kinetics were performed by immersing a blend polymeric film sample in 100 mL of aqueous surfactant solution. In all experiments, temperature was kept constant at 25.0 (±0.1) °C using a

Multistirrer 6 thermostatic bath from Velp Scientifica. During HTMA-PFP release experiments, blend-containing solutions were stirred at ca. 220 rpm. At defined intervals, 0.1 mL aliquots of the supernatant were collected. The amount of substance of HTMA-PFP released from polymeric matrices to the supernatant solution was determined by fluorescence spectroscopy, using a Jobin–Yvon SPEX Fluorolog 3-22 spectrofluorimeter in front-face configuration, with the excitation monochromator set at 381 nm, and the emission scanned between 390 and 525 nm; 2 nm excitation and emission slits were used.

3. Results and discussion

3.1. Spectroscopic and morphological analysis

The incorporation of the polyelectrolyte into cellulose acetate membranes was followed by UV–visible spectroscopy (Fig. 1). It can be seen that in the presence of the HTMA-PFP there was a significant increase in the absorbance, and, in addition, the spectra were dependent on the solvent and degree of substitution. With the exception of B1, all absorption spectra showed the characteristic poly(fluorene-phenylene) absorption band at 370 nm [14]; furthermore, HTMA-PFP in B2 exhibited a more solution-like spectrum as suggested by the absorbance peak at 414 nm. In the case of B1 a broad peak, with low absorbance, with a maximum at around 412 nm clearly suggests a more marked polymer aggregation ("solid-state-like" absorption spectrum) [33], and lack of homogeneous dispersion within the polymer blend.

From SEM micrographs (Fig. 2) it can be seen that, in contrast with the porous structures normally observed for cellulose acetate films [34], the incorporation of HTMA-PFP leads to a fairly compact, non-porous surface morphology, accompanied by phase separation in the case of commercial cellulose acetate-based blends (B1, B2 and B4). Such phase separation is clearly due to incorporation of HTMA-PFP as confirmed by FM (light blue spots in Fig. 3); it is also worthy of note that prior solubilization of HTMA-PFP in methanol (B4) leads to the formation of well-defined spherical domains with diameters up to 5 μm in the blends, as seen by SEM.

From comparison of the effect of the degree of substitution and the nature of the cellulose acetate used on the surface morphology of the blends (B2 and B3), it is possible to conclude that phase separation is also a consequence of the disruption of polyelectrolyte aggregates. In contrast to what was seen with B2 surface morphology, no surface phase separation was observed by SEM for B3.

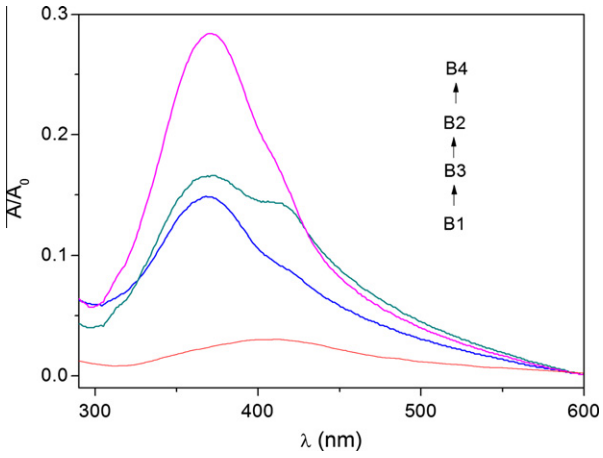

Fig. 1. UV–visible absorption spectra of CA-HTMA-PFP blend films of similar thickness.

Although no phase separation has been detected by SEM, a distribution of highly fluorescence spots was observed throughout this blend by FM (Fig. 3 – B3).

The analysis of fluorescence photograph for the blend B1 shows the absence of large aggregates (when compared, for example, with B3); this can be directly related with the low fluorescence intensity observed by FM, which can be explained by fluorescence quenching resulting from polymer aggregation [14]. This is fully consistent with the low and ill-defined UV-absorbance spectrum for B1.

To obtain deeper knowledge on the effect of the incorporation of HTMA-PFP into cellulose acetate matrices, and their potential for application in various types of device, thermal analysis techniques (TGA and DSC) were used and the data are discussed in the following sections.

3.2. Thermal stability (TGA)

The thermal stability of the different materials was studied by TGA under an nitrogen atmosphere. Table 1 shows the main thermal data obtained from the TG–DTG curves, including the temperature at which 5% of the total mass is volatilized (T_5) and temperature at the maximum degradation rate (T_{max}). T_5 provides an accurate idea of the thermal stability since the identification of the initial decomposition temperature (mass loss near to 0%) is extremely difficult because of slight variations in mass loss in this zone correspond to large temperature variations [35,36].

Fig. 4 shows TG curves for all blends with and without polyelectrolyte. A main thermal event can be seen in all cases, centred at 362 °C, that corresponds to the pyrolysis of the polymer backbone structure. In addition, there is an initial mass loss region at around 100 °C, that is likely to be associated with the loss of water in CA (also observed in DSC experiments on second heating of samples) [35].

The presence of the polyelectrolyte in the commercial CA matrices prepared in chloroform (B2 and B4) resulted in a slight decrease in T_5 (2% and 3%, respectively) and in T_{max} (2% for B2 and 1% for B4), compared with their counterparts with no polyelectrolyte. Such a decrease can be explained in terms of the mixture of non-compatible polymers, resulting in a less structured polymer network and phase separation (see Fig. 1). It should be stressed that the least affected blend upon polyelectrolyte incorporation, in terms of change of T_5, is also the one showing a less intense and broad UV/vis absorption peak (B1). In contrast, the addition of the polyelectrolyte to the synthesized CA (blend B3) resulted in an increase of T_5 (5%), suggesting some increase in the molecular order in that blend structure. The improvement in thermal stability as a function of increasing DS of CA (when comparing B2 and B3) could be explained by the formation of new-ordered structures in the substituted regions [37]. These results are in agreement with the SEM and FM images (Figs. 2 and 3).

3.3. DSC analysis

Studies of films were made by DSC on heating, cooling, and second heating cycles. A representative DSC thermogram including all heating and cooling scans of B1 sample is shown in Fig. 5. In the first heating scan, a broad endothermic band can be observed between 25 °C and 100 °C. Since this process does not appear in the second heating, it can be attributed to water desorption from CA [24,35], in complete agreement with the TG data. In the cooling step, a glass transition (T_g) can be observed, that also appears in the second heating scan just before melting transitions for all samples.

Fig. 6 shows the DSC curves of CA-HTMA-PFP films during the second heating scan, after erasing the thermal history of the samples. Samples with commercial CA1 (B1, B2 and B4) showed

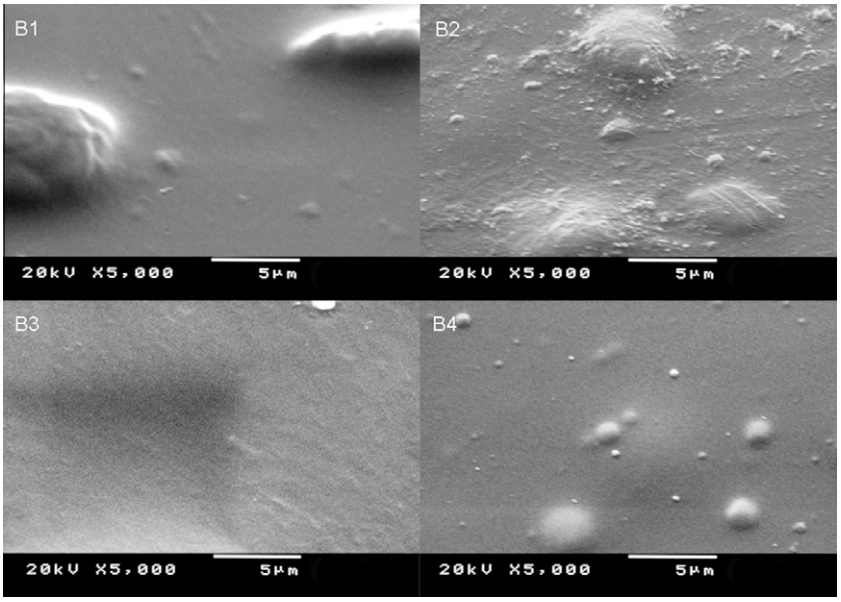

Fig. 2. SEM micrographs of the surface of cellulose acetate-HTMA-PFP blends.

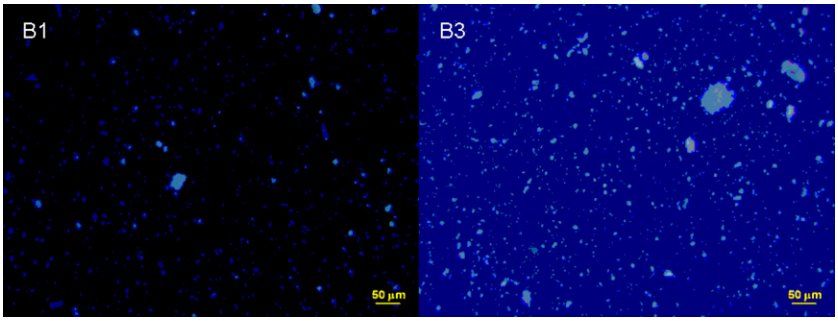

Fig. 3. Fluorescence microscopy photographs of cellulose acetate-HTMA-PFP blends.

Table 1
Thermal parameters of cellulose acetate and cellulose acetate-HTMA-PFP polymers, determined by TGA.

Film	T_5 (°C)	T_{max} (°C)
B1	317 (315)	362 (361)
B2	304 (310)	356 (364)
B3	332 (317)	365 (362)
B4	304 (314)	359 (364)

T_5: Temperature when 5% of the total mass is volatized, determined from TGA curves.
T_{max}: temperature determined from the maximum of DTG curves.
Values inside brackets are obtained for cellulose acetates without polyelectrolyte.

endothermic transitions just after glass transition due to the melting of the crystalline structure of cellulose acetate.

It should be noted that B3 showed different behavior from the other blends. It was the only one showing an exothermic transition peak at 209 °C corresponding to crystallization and a broad melting peak at higher temperatures (around 260 °C). The ability of the cellulose acetate, obtained from sugarcane bagasse (CA2), to crystallize from amorphous structures during DSC upon heating, could explain this exothermic transition. The amplitude of this peak is normally dependent on the degree of substitution, since higher DS values lead to more homogeneous chains and, consequently, better chain packing and greater crystallinity. In agreement with this, CA2 (DS = 2.6) is characterized by melting at higher temperatures than CA1 (DS = 2.4) because of its higher degree of substitution. Another explanation for this thermal behavior can be found in the chain length, as measured by the degree of polymerization of the materials, since CA2 has a lower DP value than CA1, which allows better structure packing [24].

To study the effect of the addition of polyelectrolyte and the use of different solvents on the thermal behavior of the various CA blends, glass transition temperatures and total enthalpy values were obtained from the second heating scan, and are summarized in Table 2. For blends B1, B2 and B4, the total enthalpy (ΔH_{total}) corresponds to the melting process (approximately between 200 °C and 230 °C). In the case of blend B3, the baseline integration peak used to calculate ΔH_{total} was taken from the beginning of crystallization process to the final of the melting transition [24].

It can be seen that the lowest T_g value corresponds to B3, where the cellulose acetate used in this sample (CA2) has a lower molar mass and higher DS than CA1. This result and our T_g values are in agreement with the literature on related systems [37]. In general, the incorporation of 2 wt.% of HTMA-PFP in cellulose acetate films did not induce a significant decrease in T_g values.

As already mentioned, in B3, the higher polymerization degree of the cellulose acetate (CA2) is what controls the crystallization and melting processes and is likely to be the reason for the higher ΔH_{total} value (and higher crystallinity) of this blend compared with those based on commercial CA (B1, B2 and B4). These blends

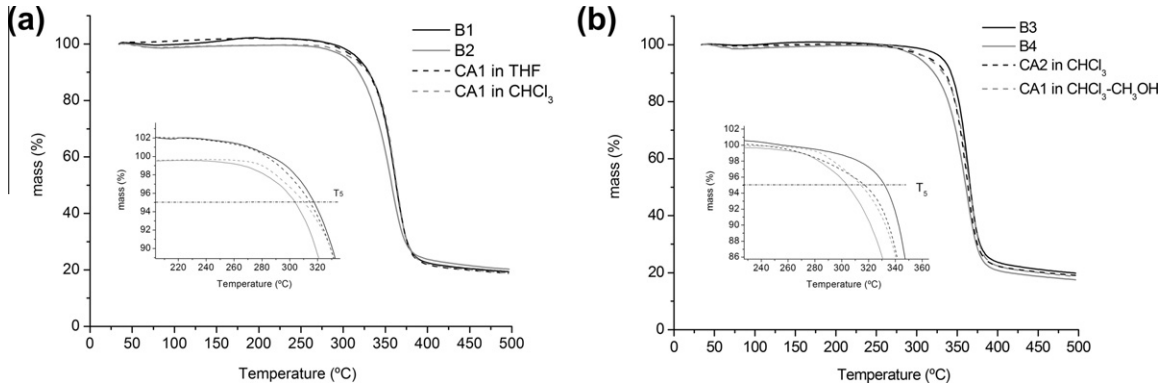

Fig. 4. TG curves of B1–B2 (a) and B3–B4 (b) comparison with the corresponding cellulose acetate without polyelectrolyte (dash lines).

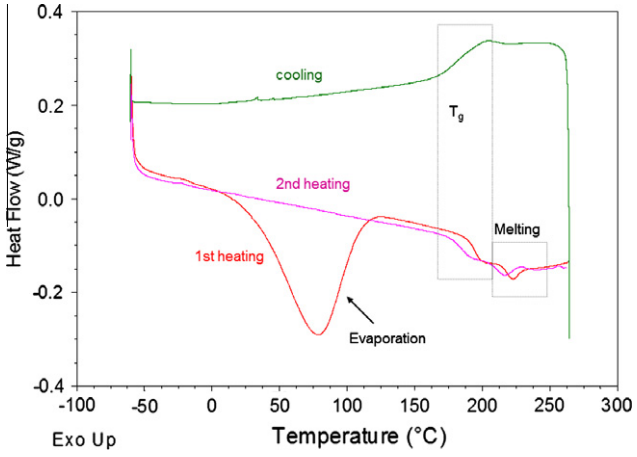

Fig. 5. DSC thermogram for B1 (CA1-HTMA-PFP) sample displaying the heating and cooling ramps at 10 °C min^{-1}.

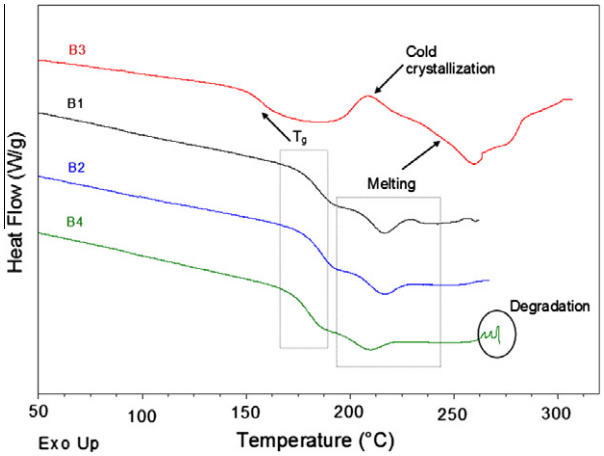

Fig. 6. DSC thermograms for cellulose acetate-HTMA-PFP films during the second heating scan at 10 °C min^{-1}.

showed similar ΔH_{total} values without polyelectrolyte but the incorporation of HTMA-PFP resulted in a decrease of about 20% in the ΔH_{total} values, and, consequently, reflect a decrease in the chain packing and in polymer crystallinity. No differences were observed in DSC behavior on use of different solvents for film preparation, or by the previous solubilization of the polyelectrolyte. However, the presence of HTMA-PFP in blend B3 produced an increase of about 50% in the ΔH_{total} value, increasing the polymer crystallinity, and is consistent with the homogeneous distribution and compacted structure observed by SEM and FM after incorporation of polyelectrolyte. It is also worthy of note that changes in the polymer structures, as suggested from the DSC data, were also supported by electrical conductivity measurements. The semi-crystalline polymer structure of cellulose acetate with DS = 2.6 (B3) showed a very small electrical conductivity (0.3 μS cm^{-1}) and no effect on the value of κ was observed upon incorporation of HTMA-PFP. However, in blends of commercial cellulose acetate, a significant increase in the electrical conductivity was observed compared with B3, and is probably related to the lower crystallinity of these samples. Also, the incorporation of HTMA-PFP in these blends leads to an increase of around 50% in the electrical conductivity values (from 6.0 to 12.1 μS cm^{-1} for B1, from 6.8 to 23.8 μS cm^{-1} for B2 and from 4.5 to 8.1 μS cm^{-1} for B4), and is in agreement with the decrease in crystallinity observed in DSC.

Table 2
Glass transition temperatures (T_g) and total enthalpies ΔH_{total} calculated from DSC curves (second heating) of cellulose acetate (inside brackets) and cellulose acetate-HTMA-PFP polymers.

Film	T_g (°C)	ΔH_{total} (J/g)
B1	183.7 (185.1)	2.3 (2.8)
B2	185.9 (186.7)	2.1 (2.8)
B3	157.9 (158.8)	5.0 (3.2)
B4	180.0 (188.9)	2.5 (3.0)

Even though they are small in absolute terms, these values give good indications of the advantages in the development of matrices with higher polyelectrolyte content, which can thus be used to tune the ionic electrical conductivity of these matrices. This is likely to be of value in device design for sensing and optoelectronic applications.

3.4. Release of HMTA-PFP from cellulose acetate-based blends

As was indicated in the introduction, low solubility in water is one important limitation of the conjugated polyelectrolyte HTMA-PFP for many practical applications. There are several strategies to overcome this difficulty: one is the use of the polymer in a solid matrix, while a second is to find out various ways of dispersing or dissolving the polyelectrolyte in appropriate aqueous solution. It is known that the solubility of HTMA-PFP in water increases in the presence of surfactants [30,33]. The release kinetics of HTMA-PFP from blend films into surfactant solutions are expected to give relevant information, both concerning the nature of

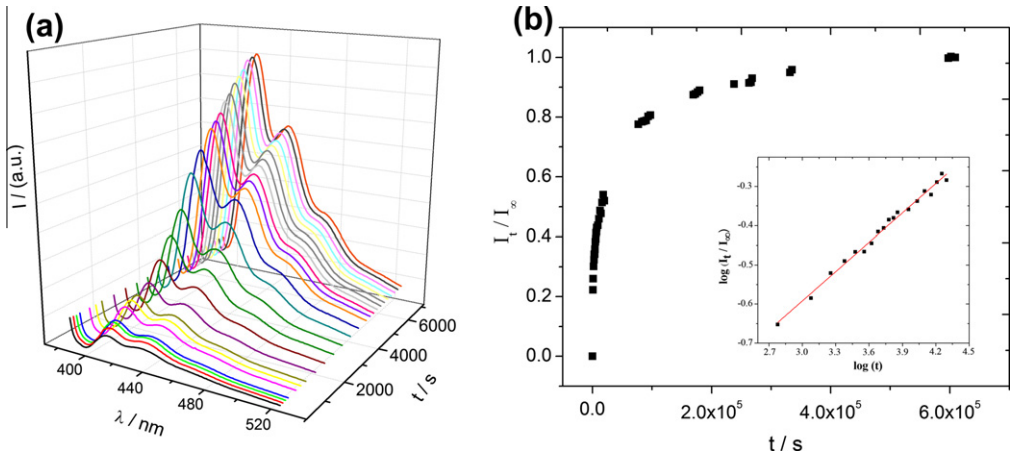

Fig. 7. Representative fluorescence emission spectra (a) and normalized release kinetics (b) of HTMA-PFP from B2 to 12 mM SDS aqueous solutions at 25 °C.

physical or chemical mechanisms involved for incorporation into the matrix, and also on possible novel applications for, e.g., sensing.

In this section, the effect of aqueous solutions of the anionic SDS on the release properties of HTMA-PFP from the different blends at surfactant concentrations (12 mM) above the cmc is analyzed and discussed. Release experiments were also carried out with pure water and with aqueous 6 mM SDS solutions. In neither of these two cases was there any evidence for desorption to the liquid phase after 2 weeks, as shown by the absence of HTMA-PFP in solution, monitored by fluorescence spectroscopy.

Fig. 7a shows representative fluorescence emission spectra of HTMA-PFP desorbed from cellulose acetate films into 12 mM SDS solution at different times. The plot of the maximum emission intensity at 417 nm vs. time (Fig. 7) allows the evaluation of the kinetic rate constant and desorption mechanism.

A number of equations have been developed to model the sorption/desorption kinetics of diffusing species from polymeric matrices, ranging from those based on purely theoretical models [38] to semi-empirical approaches [39].

The classical one among these is the Korsmeyer–Peppas equation [40]

$$C_t/C_\infty = kt^n \quad (1)$$

where C_t and C_∞ are cumulative concentrations of the material released at time t and at infinite time, respectively, and k and n are fitting parameters. If the exponent n is 0.5 (for planar systems) the diffusion is Fickian. Non-Fickian behavior is observed for $0.5 < n < 1.0$, with a limit of Case II transport for $n = 1.0$. Non-Fickian and Case II transport are indicative of coupling of diffusional and relaxational mechanisms. However, the validity of Eq. (1) is restricted to $C_t/C_\infty < 0.60$ [41]).

In the present study, the concentration ratio C_t/C_∞ was considered as equal to the ratio of the emission fluorescence intensity at time t and at infinite time, I_t/I_∞. Table 3 summarizes the parameters obtained from a non-linear least-square fitting of Eq. (1) to the experimental release data. It can be seen that B1 shows an anomalous mechanism, indicating that coupled diffusion/polymer relaxation takes place; however, in the case of B2 and B4, with both blends prepared using $CHCl_3$ as the main solvent, n values were less than 0.5 (0.25 and 0.38, respectively). Such values have previously been reported for other systems [e.g., 42], and they have been taken to imply that diffusion is the dominant mechanism (so-called quasi-Fickian) of HTMA-PFP release. In the case of B3, however, the HTMA-PFP release mechanism was only dependent on the concentration gradient (so-called Fickian). Consequently,

Table 3
Parameters computed from fitting the experimental HTMA-PFP release to Eq. (1), at 25 °C.

	Eq. (1)		
	$\log k$	n	R^2
B1	−3.51 (±0.09)	0.86 (±0.03)	0.9763
B2	−1.34 (±0.02)	0.250 (±0.006)	0.9906
B3	−2.43 (±0.02)	0.480 (±0.006)	0.9972
B4	−1.87 (±0.03)	0.379 (±0.008)	0.9920

the diffusion coefficient, D, of HTMA-PFP can be calculated using the Eq. (2)

$$D = \left(\frac{kl\pi^{1/2}}{4}\right)^2 \quad (2)$$

where l is the thickness of membrane, and gives a value of 5.42×10^{-10} cm^2 s^{-1}. This diffusion coefficient is four orders of magnitude lower than those obtained for this polyelectrolyte in DMSO/H_2O solutions (ca. 4×10^{-6} cm^2 s^{-1}) [43]. As discussed in Section 3.1, B3 shows a greater compaction (when compared with other blends), resulting from the lowest polymerization degree of the cellulose acetate. As a consequence, the resistance of the blend to the transport of HTMA-PFP is likely to increase [44] leading to a slow diffusion process.

Although no definitive conclusions about the dependence of the release mechanism on the structural properties of blends can be extracted, a reasonable hypothesis is that the solvent used for film casting plays an important role on the structure of both, cellulose acetate and HTMA-PFP; furthermore it is worth noting that the anomalous mechanism of release occurs in the blend where the UV–visible spectrum suggests the occurrence of a highly aggregated structure.

4. Conclusions

Blends of HTMA-PFP and cellulose acetate, with different degrees of substitution, have been prepared from various solvents (THF, $CHCl_3$ and $CHCl_3/CH_3OH$). The morphology, fluorescence and transport properties of blends films are dependent on the composition. The blend based on cellulose acetate with the lowest polymerization degree shows no surface phase separation and strong fluorescence; furthermore, this blend also shows the highest thermal stability, while the desorption of HTMA to SDS follows a Fickian diffusion mechanism with the lowest release rate; the use

of $CHCl_3$ as casting solvent leads to highly fluorescent amorphous structures; in this case, the previous dissolution of HTMA-PFP in CH_3OH gives an excellent method to reduce the aggregation of the polyelectrolyte and, thus, increase the UV–visible absorption; in addition, it leads to a release rate one order of magnitude higher than those found to other blends; it is worth noticing that such a release rate can also be affected by relaxation/mobility of the polymeric structure responsible for the anomalous mechanism of the HTMA-PFP transport. With this work we have demonstrated that polyelectrolyte-containing cellulose acetate blends with different properties can be prepared, and since it is possible to control their properties by changing the solvent and/or the degree of substitution of cellulose acetate, they have potential for a wide variety of applications, ranging from sensing to controlled release.

Acknowledgments

Financial support from CRUP (Project E-1/09) and Spanish Ministry of Science and Innovation (Projects HP-2008-0080, PT-2009-0002 and MAT-2008-05670) are gratefully acknowledged.

References

[1] A. Duarte, K.-Y. Pu, B. Liu, G.C. Bazan, Chem. Mater. 23 (2011) 501–515.
[2] B.Q. Bao, L. Yuwen, X.W. Zhan, L.H. Wang, Polym. Sci. Part A: Polym. Chem. 48 (2010) 3431–3439.
[3] M.J. Tapia, M. Monteserín, A.J.M. Valente, H.D. Burrows, R. Mallavia, Adv. Colloid Interf. Sci. 158 (2010) 94–107.
[4] M.L. Davies, H.D. Burrows, S. Cheng, M.C. Morán, M.G. Miguel, P.D. Douglas, Biomacromolecules 10 (2009) 2987–2997.
[5] W.L. Ma, P.K. Iyer, X. Gong, B. Liu, D. Moses, G.C. Bazan, A.J. Heeger, Adv. Mater. 17 (2005) 274–277.
[6] C. Hoven, R. Yang, A. Garcia, A.J. Heeger, T.Q. Nguyen, G.C. Bazan, J. Am. Chem. Soc. 129 (2007) 10976–10977.
[7] L.T. Ho, F. Huang, J.B. Peng, H.B. Wu, S.S. Wen, Y.Q. Mo, Y. Cao, Thin Solid Films 515 (2006) 2632–2634.
[8] G. Decher, Science 277 (1997) 1232–1237.
[9] U.S. Schubert, Macromol. Rapid Commun. 26 (2005) 237.
[10] R. Rulkens, G. Wegner, T. Thurn-Albrecht, Langmuir 15 (1999) 4022–4025.
[11] U. Scherf, E.J.W. List, Adv. Mater. 14 (2002) 477–487.
[12] H.D. Burrows, V.M.M. Lobo, J. Pina, M.L. Ramos, J. Seixas de Melo, A.J.M. Valente, M.J. Tapia, S. Pradhan, U. Scherf, Macromolecules 37 (2004) 7425–7427.
[13] H.D. Burrows, M. Knaapila, A.P. Monkman, M.J. Tapia, S.M. Fonseca, M.L. Ramos, W. Pyckhout-Hintzen, S. Pradhan, U. Scherf, J. Phys.: Cond. Matter 20 (2008) 102410.
[14] M. Monteserín, H.D. Burrows, A.J.M. Valente, V.M.M. Lobo, R. Mallavia, M.J. Tapia, I.X. García–Zubiri, R.E. Di Paolo, A.L. Maçanita, J. Phys. Chem. B 111 (2007) 13560–13569.
[15] H.D. Burrows, M.J. Tapia, S.M. Fonseca, S. Pradhan, U. Scherf, C.L. Silva, A.A.C.C. Pais, A.J.M. Valente, K. Schillen, V. Alfredsson, A.M. Carnerup, M. Tomsic, A. Jamnik, Langmuir 25 (2009) 5545–5556.
[16] P. Sarrazin, L. Valecce, D. Beneventi, D. Chaussy, L. Vurth, O. Stephan, Adv. Mater. 19 (2007) 3291–3294.
[17] B.Q. He, J. Li, Z.S. Bo, Y. Huang, J. Appl. Polym. Sci. 106 (2007) 1390–1397.
[18] S.P. Liu, L.J. Tan, W.L. Hu, X.Q. Li, Y.M. Chen, Mater. Lett. 64 (2010) 2427–2430.
[19] A.J.M. Valente, H.D. Burrows, A.Y. Polishchuk, C.P. Domingues, O.M.F. Borges, M.E.S. Eusébio, T.R. Maria, V.M.M. Lobo, A.P. Monkman, Polymer 46 (2005) 5918–5928.
[20] Z.M. Mao, Y.M. Cao, X.M. Jie, G.D. Kang, M.Q. Zhou, Q. Yuan, Sep. Purif. Technol. 72 (2010) 28–33.
[21] H.A. Gulec, A. Topacli, C. Topacli, N. Albayrak, M. Mutlu, J. Membr. Sci. 350 (2010) 310–321.
[22] D. Zavastin, I. Cretescu, M. Bezdadea, M. Bourceanu, M. Drăgan, G. Lisa, I. Mangalagiu, V. Vasić, J. Savić, Colloids Surf. A: Physicochem. Eng. Asp. 370 (2010) 120–128.
[23] F. Fischer, A. Rigacci, R. Pirard, S. Berthon-Fabry, P. Achard, Polymer 47 (2006) 7636–7645.
[24] H.S. Barud, A.M. de Araujo, D.B. Santos, R.M.N. Assunção, C.S. Meireles, D.A. Cerqueira, G.R. Filho, C.A. Ribeiro, Y. Messaddeq, S.J.L. Ribeiro, Thermochim. Acta 471 (2008) 61–69.
[25] D.A. Cerqueira, A.J.M. Valente, G.R. Filho, H.D. Burrows, Carbohydr. Polym. 78 (2009) 402–408.
[26] G.R. Filho, S.F. da Cruz, D. Pasquini, D.A. Cerqueira, V.D.S. Prado, R.M.N. Assunção, J. Membr. Sci. 177 (2000) 225–231.
[27] D.A. Cerqueira, G.R. Filho, R.A. Carvalho, A.J.M. Valente, Polimeros 20 (2010) 85–91.
[28] R. Mallavia, D. Martinez-Peréz, B.F. Chmelka, G.C. Bazan, Bol. Soc. Esp. Ceram. Vidr. 43 (2004) 327–330.
[29] H.D. Burrows, S.M. Fonseca, C.L. Silva, A.A.C.C. Pais, M.J. Tapia, S. Pradhan, U. Scherf, Phys. Chem. Chem. Phys. 10 (2008) 4420–4428.
[30] A. Gutacker, N. Koenen, U. Scherf, S. Adamczyk, J. Pina, S.M. Fonseca, A.J.M. Valente, R.C. Evans, J.C. Melo, H.D. Burrows, M. Knaapila, Polymer 51 (2010) 1898–1903.
[31] S. Nouri, L. Dammak, G. Bulvestre, B. Auclair, Eur. Polym. J. 38 (2002) 1907–1913.
[32] K. Holmberg, B. Jönsson, B. Kronberg, B. Lindman, Surfactants and Polymers in Aqueous Solution, second ed., Wiley, Chichester, 2003.
[33] H.D. Burrows, M.J. Tapia, S.M. Fonseca, A.J.M. Valente, V.M. M Lobo, L. Justino, S. Qiu, S. Pradhan, U. Scherf, N. Chattopadhyay, M. Knaapila, V. Garamus, ACS Appl. Mater. Interf. 1 (2009) 864–874.
[34] A.J.M. Valente, A.Y. Polishchuk, H.D. Burrows, V.M.M. Lobo, Eur. Polym. J. 41 (2005) 275–281.
[35] A. Martínez-Felipe, E. Ballester-Sarrias, C.T. Imrie, A. Ribes-Greus, J. Appl. Polym. Sci. 115 (2010) 3282–3294.
[36] F. Carrasco, P. Pagès, J. Gámez-Pérez, O.O. Santana, M.L. Maspoch, Polym. Degrad. Stab. 95 (2010) 116–125.
[37] L.C. Fidale, C. Issbrucker, P.L. Silva, C.M. Lucheti, T. Heinze, O.A. El Seoud, Cellulose 17 (2010) 937–951.
[38] J. Crank, The Mathematics of Diffusion, second ed., Oxford University Press Inc., New York, 1975.
[39] B. Amsden, Mech. Models Macromol. 31 (1998) 8382–8395.
[40] R.W. Korsmeyer, R. Gurny, E. Doelker, P. Buri, N.A. Peppas, Int. J. Pharm. 15 (1983) 25–35.
[41] P.L. Ritger, N.A. Peppas, J. Control. Release 5 (1987) 23–26.
[42] J.F. Piai, L.C. Lopes, A.R. Fajardo, A.F. Rubira, E.C. Muniz, J. Mol. Liq. 156 (2010) 28–32.
[43] M. Monteserin, M.J. Tapia, A.C.F. Ribeiro, C.I.A.V. Santos, A.J.M. Valente, H.D. Burrows, R. Mallavia, M. Nilsson, O. Söderman, J. Chem. Eng. Data 55 (2010) 1860–1866.
[44] A.J.M. Valente, H.D. Burrows, A.Y. Polishchuk, M.G. Miguel, V.M.M. Lobo, Eur. Polym. J. 40 (2004) 109–117.